

Monitoring of drinking water quality using automated ATP quantification

Hansen, C.B.¹, Kerrouche, A.², Tatari, K.¹, Rasmussen, A.¹, Ryan, T.³, Summersgill, P.³, Desmulliez, M.P.Y.⁴, Bridle, H.⁵ and Albrechtsen, H.J.¹

1. Technical University of Denmark, Lyngby, Denmark.
2. Napier University, Edinburgh, Scotland, UK.
3. Epigem, Redcar, UK.
4. Multi-Modal Sensing and Micro-Manipulation Centre (CAPTURE); Institute of Sensors, Signals and Systems (ISSS); Heriot-Watt University, Edinburgh EH14 4AS, Scotland, UK.
5. Institute of Biological Chemistry, Biophysics and Bioengineering; Heriot-Watt University, Edinburgh EH14 4AS, Scotland, UK.

Abstract: A microfluidic based system was developed for automated online method for the rapid detection and monitoring of drinking water contamination utilising microbial Adenosine-5'-Triphosphate (ATP) as a bacterial indicator. The system comprises a polymethyl methacrylate based microfluidic cartridge inserted into an enclosure incorporating the functions of fluid storage and delivery, lysis steps and real-time detection. Design, integration and operation of the resulting automated system are reported, including the lysis method, the design of the mixing circuit, the choices of flow rate, temperature and reagent amount. Calibration curves of both total and free ATP were demonstrated to be highly linear over a range from 2.5-5,000 pg/mL with the limit of detection being lower than 2.5 pg/mL of total ATP. The system was trialled in a lab study with different types of water, with lysis efficiency being found to be strongly dependent upon water type. Further development is required before online implementation.

Keywords: microfluidics, drinking water, microbial contamination, monitoring, ATP

I. Introduction

Monitoring the quality of drinking water confirms the success of treatment systems, and the integrity of distribution networks, in the delivery of pathogen-free water. Most of the current testing of faecal indicators undertaken by water utilities is lab-based, time consuming and requires culturing, preventing therefore real-time warning of presence of pathogens. To combat these limitations, development of online methods has accelerated, with commercially available systems [1] as well as trial set-ups being adopted in water systems worldwide for source water surveillance [2] and distribution network quality control [3]. Microbial water quality monitoring systems based on optical, electrical or molecular methods of detection have all been developed, though not all have suitability for online or early-warning approaches [4]. For early-warning systems a variety of

36 approaches have been tested ranging from the utilisation of online measurements of conductivity
37 and/or turbidity as a proxy [5] to automated culture based systems, online flow cytometry platforms
38 [6], particulate imaging using 3D scanning [7], microbiome analysis [8] and use of indicators such as
39 tryptophan [9] or adenosine-5'-triphosphate (ATP) [10]. ATP was recently found to be the most
40 accurate approach in a comparison of three different sensor types [11].

41 ATP measurements are widely used in the analysis of microbial contamination in a variety of
42 industries [12], including the water industry [3]. Total ATP in drinking water is the sum of microbial
43 ATP (in active and viable cells) and free ATP. , An ATP assay will be able to detect either total ATP if
44 an extraction reagent is used, or free ATP only without this reagent. The microbial ATP content can
45 therefore be calculated as the difference between these two measurements. Recent work has
46 highlighted the utility of ATP in detecting microbial ingress in drinking water by demonstrating that
47 the approach was more sensitive than total direct counts and more rapid than culture based
48 methods such as heterotrophic plate counts and Colilert-18 [10]. However, the system was used in a
49 benchtop batch processing setup which is bulky and laboratory based. As a proven fast and reliable
50 technique, online integration of ATP quantification for drinking water quality would be a very useful
51 tool, (e.g. Applitek [13]).

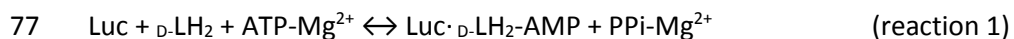
52 Microfluidics refers to the design, manufacture and testing of systems capable of manipulating and
53 transporting tiny volumes of water with channel dimensions in the order of micrometres.
54 Microfluidic technologies have been applied to numerous biological and biomedical challenges,
55 including water quality monitoring [14]. The advantages of microfluidics are precise, automated
56 control over reagent addition and mixing, an on-chip analysis and measurement approach avoiding
57 human error or contamination and a small, portable device using small quantities of expensive
58 reagents per measurement. Microfluidics has been utilised for ATP detection; specifically,
59 microfluidics-based ATP devices have been reported for submetabolomic analysis [15], detecting
60 airborne microorganisms [16] and for sea water monitoring [12, 17]. For water quality applications *E.*
61 *coli* O157:H7 detection was reported by integration of the ATP assay with immunomagnetic
62 separation [18] and a paper based microfluidic system was used with *Salmonella* [19]. Here, we
63 report on the development and optimisation of a microfluidic device, integrated into a detection
64 system, for ATP quantification for drinking water quality applications. The focus of the paper is on
65 the design and operation of the system and the impact of lysis protocol on device performance in lab
66 studies. Additionally, unlike in the previous systems, detection of both total and free ATP has been
67 investigated.

68

69 II. Materials and Methods

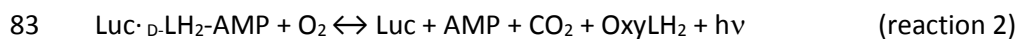
70 ATP Detection Assay:

71 ATP is most commonly measured by a chemiluminescence assay (Luc assay). The first step of the
72 assay is the extraction of ATP from the cells by lysis reagents (typically cold extractants) [3, 20, 21].
73 The extracted ATP is then quantified by a two-step reaction that uses the firefly luciferase enzyme
74 (Luc) and its substrate luciferin ($D\text{-LH}_2$). The bioluminescence is also dependent on the oxygen (O_2)
75 concentration and the presence of Mg^{2+} that leads to the formation of the ATP- Mg^{2+} complexes as
76 illustrated in reactions 1 and 2 [22].



78 Where $\text{Luc}\cdot D\text{-LH}_2\text{-AMP}$ (D -luciferil-adenylate) is the enzyme-bound intermediate generated after the
79 hydrolysis of ATP to AMP (adenosine monophosphate), and PPI-Mg^{2+} is the inorganic pyrophosphate
80 ($P_2O_7^{4-}$) bound to Mg^{2+} .

81 In the second reaction, the intermediate $\text{Luc}\cdot D\text{-LH}_2\text{-AMP}$ is oxidized and decarboxylized, emitting light
82 whose intensity is proportional to the initial ATP content [22]:



84 Where OxyLH_2 (oxyluciferin) is the light emitting molecule and $h\nu$ is the energy of the emitted
85 photons whose wavelength lies in the yellow-green spectrum. The light emission reaches its
86 maximum intensity within a second, after which it decreases depending on the assay conditions and
87 the luciferase concentration [23]. Low luciferase concentrations give a relatively stable light
88 emission, while high luciferase concentrations, also known as flash reagents, give light emission that
89 lasts for a very short time. The bioluminescence reaction is particularly sensitive to pH and
90 temperature. The optimal reaction temperature is 25°C [24] whilst the optimal pH during the assay is
91 between 6 and 8 [23] and is controlled by buffer addition. The luciferin-luciferase reagents were the
92 LuminATE kit (92687, Celsis).

93 Microfluidic Design, Microfabrication and Operation:

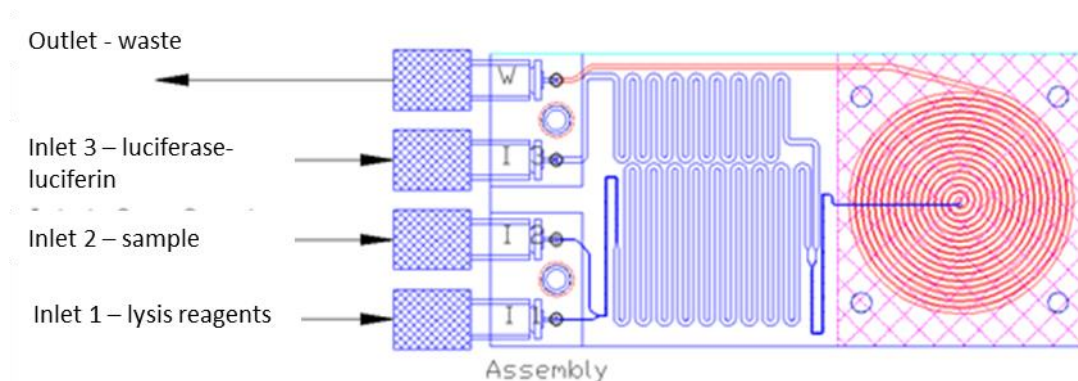
94 In similarity to ATP detecting microfluidic systems created by Lee [16] and Fukuba [12] the device is
95 composed of a mixing zone for the various liquids, a detection area and several inlets to introduce
96 the sample, lysis agent and detection reagents. More specifically, from left to right in Figure 1, the
97 sample and reagents are introduced from their storage flasks to inlet channels in the microfluidic
98 system via semi-rigid tubing (Cheminert®). Two sequential mixing sections made of serpentine
99 channels ensure the efficient combination of the sample with the lysis reagent (liquids from inlets 1

100 and 2), and of the lysed sample with the chemiluminescence reagents (output of first mixing section
101 with liquid from inlet 3). The reagents require storage at 4°C degrees to preserve their reactivity and
102 shelf life. The long serpentine channels with the microfluidic device have therefore also been
103 designed to allow time for the liquids to reach the optimal reaction temperature for the Luc
104 reaction. Finally, the sample enters a detection zone in which the channel forms a 32 mm diameter
105 spiral. The spiral shape ensures maximum capture of the luminescent signal from the samples. To
106 ensure the produced light is reflected towards the detector a metallic layer of foil was placed
107 externally below the device and opposite the spiral. Two different mixing designs were trialed and
108 assessed via imaging (Dinolite) of the mixing of food dye.

109 The microfluidic system was manufactured by Epigem Ltd using acrylic (PMMA) and epoxy. The
110 choice of materials was based on the requirement for long term robustness, good compatibility with
111 wet conditions in the device and good light transmission in 550-650 nm wavelength produced by the
112 Luc reaction.

113 Sample and reagents were supplied to the microfluidic device inlets using a peristaltic pump
114 (ISMATEC Reglo ICC). After calibration, the pump displayed a maximum 5% deviation from the
115 nominal flow rate. The 0.51 mm inner diameter pumping tube used for the peristaltic pumps was
116 made from a silicone based polymer and was linked to a 0.2 mm inner diameter and 1.59 mm outer
117 diameter small bore analytical semi-rigid tubing (Cheminert) to minimise the volume of expensive
118 reagents used (31 μL per meter of tubing). Further reduction of volume was carried out using short
119 length connections from the pumping tube to the reagents and sampling reservoirs next to the
120 pump as well as the microfluidic inlets. Two-way pinch valves with an internal volume of 14 μL (NI
121 USB 6525 from National Instruments), were selected to control the flow of reagents and solution.
122 and are electrically actuated using controllable solid state relays.

123
124



125
126

Figure 1: Overview of the design and operation of the microfluidic system.

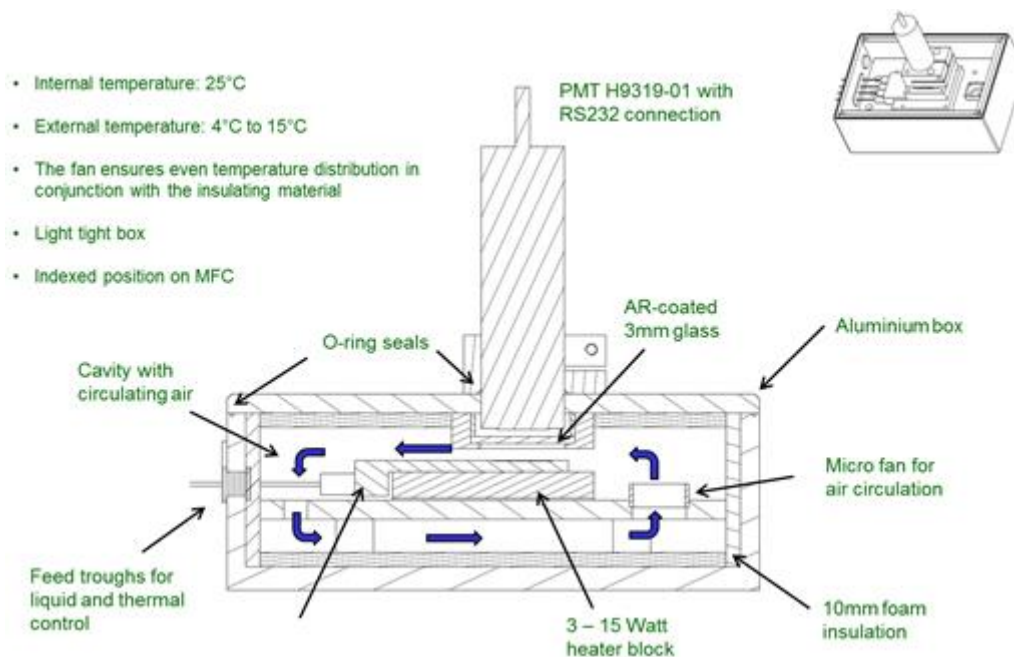
127

128 System Setup:

129 This mixing and detection system, whose schematic is displayed in Figure 2, is contained within a
130 light-tight box. The box is thermally insulated and includes a temperature control system for
131 constant temperature of 25°C to ensure stable and optimal temperature condition for the Luc
132 reaction. A small fan is also employed to avoid any gradient of temperature inside the box. The
133 temperature of an aluminium plate is regulated using an electrical heater fitted on the underside of
134 the plate. The temperature of the plate is measured by a K-type thermocouple sensor on the side of
135 the plate and the signal is used by a PID controller to maintain the desired temperature. The
136 precision of the regulating loop is within $\pm 0.1^\circ\text{C}$, and the temperature can be set in the interval from
137 the surrounding temperature of the detection box up to 36°C. A 3 mm thick, 98% total light
138 transmission, anti-reflection coated glass was inserted between the head of the Photo-Multiplier
139 Tube (PMT) and the microfluidic device to avoid the heating up of the light sensitive coating of the
140 detector.

141 A H9319-01 Hamamatsu PMT detector was selected as it offers very effective in-built amplification
142 of low light intensity signals for easier detection, the right spectral response (550 nm-650 nm) of the
143 photosensitive material inside the detector as well as a low level of thermal noise. The spiral
144 readout area on the microfluidic device was made slightly larger, with a diameter of \varnothing 32 mm, to
145 ensure full use of the \varnothing 22 mm diameter detector area rather than trying to minimize the volume of
146 the spiral.

147 The PMT detector and the centre of the spiral are placed on the same longitudinal axis, with the
148 PMT mounted in the lid of the assay box as shown in Figure 2. The tubing and the electrical wires
149 enter the box through tight rubber gaskets that prevent light from entering the detection box.



150

151

Figure 2: Schematic of the design of the whole mixing and detection system.

152

153 System Evaluation:

154 ATP standard salt (92638, Celsis) was reconstituted in Lumin (PM) buffer (92678, Celsis), MilliQ-
 155 water or sterile filtrated autoclaved drinking water at a concentration of 1×10^6 pg ATP/mL and
 156 stored at 1°C. Dilutions were then made using autoclaved, sterile filtered tap water (i.e. ATP free)
 157 for standards experiments in the range 2.5-500 pg/mL. Subsequently, the system was tested with
 158 different water types (collected at DTU). The wastewater utilised was diluted 100 times before use.
 159 The rainwater sample was collected after storage in a tank for 3 weeks. The tap water sample was
 160 taken from the lab tap during the middle of the day, and after a preliminary measurement where
 161 low levels of ATP were measured the ATP standard salt was used to spike the sample for the study
 162 evaluating different lysis approaches.

163

164 III. Results and Discussion

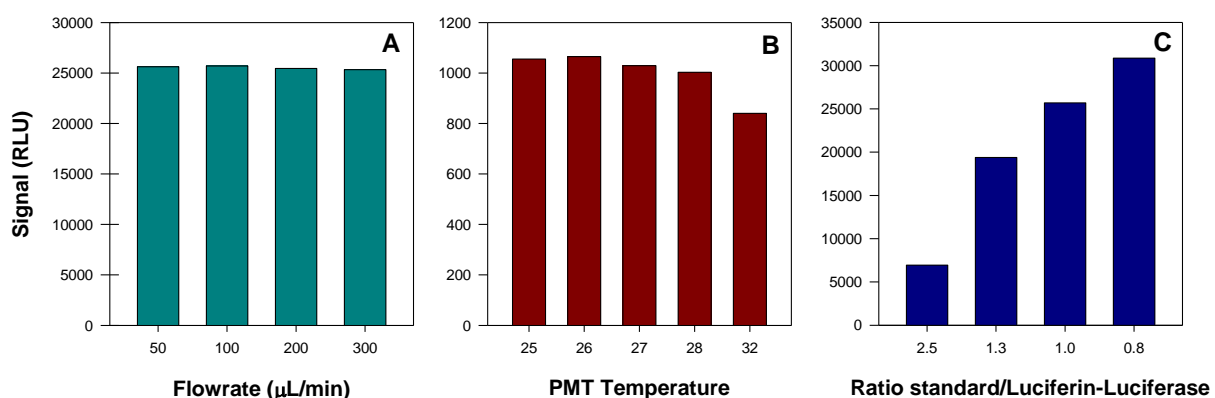
165

166 A. ATP Detection and Calibration

167 Using a 1000 pg/mL ATP standard, the impact of operating conditions on the obtained optical signal
 168 was investigated with flow rates ranging from 50 μ L/min to 300 μ L/min and temperatures between
 169 25°C and 32°C. As shown in Figure 3A, flow rates within the studied range have no impact upon the
 170 output signal whereas temperatures above 28°C result in a small decrease in the signal with results

171 being similar between 25°C and 27°C (Figure 3B). The optimal temperature of 25°C for the Luc
172 reaction is also confirmed. Different ratios of sample to luciferin-luciferase reagents were also
173 tested, as shown in Figure 3C, to explore the possibility of reducing the amount of enzyme required
174 for detection. Unsurprisingly, Figure 3C shows that the greater amount of reagent is employed, the
175 higher the obtained signal. From these three results, operating conditions of 100 µL/min, 25°C and a
176 1:1 ratio of sample/reagent were selected.

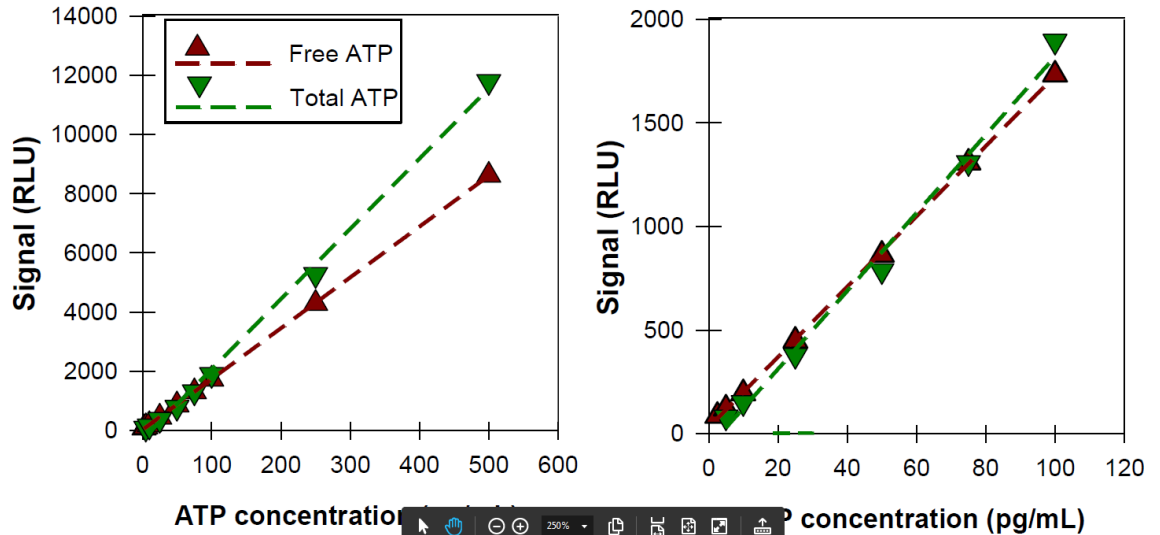
177 Calibration curves for the PMT detector were obtained using the optimised detection parameters
178 described above for both total and free ATP detection as well as determination of the limit of
179 detection. These curves are essential to convert the signals expressed in Relative Light Units (RLU)
180 into pg/mL concentrations and to account for any possible inhibition or quenching caused by the
181 lysis reagent. Two series of nine standards in the 2.5-500 pg/mL ATP concentration range were run
182 to obtain the calibration curves for total and free ATP as shown in Figure 4. Indicative peak
183 responses of the standards and peak decrease back to the background levels after the injection of
184 the standards are shown in the Supplementary Information (Figure S2). The two calibration curves
185 fitted well into a linear model ($R^2 = 0.997$ for total and $R^2 = 1$ for free ATP). The lowest standard, 2.5
186 pg/mL, is within the noise for the total ATP calibration curve and provides a signal to noise ratio
187 (SNR) of 1.5:1 for the free ATP calibration curve. This result indicates that the limit of detection is
188 better than 2.5 pg/mL, a slight improvement over the previously reported microfluidic ATP analyser
189 [12]. This is also significantly lower than the paper based device reported in 2015 although the paper
190 system did not use a PMT detector [19].



191
192

193 Figure 3: Characterisation of operational parameters for detection expressed as Relative
194 Light Units (RLU). A) Impact of varying flow rates. B) Effect of varying temperatures in the
195 PMT stage. C) Influence on the output signal of the luciferin-luciferase reagent for detection.

196



197
 198 Figure 4: Calibration curves for both total and free ATP. Figure on the left shows the entire
 199 investigated range whereas the figure on the right is a magnified view of the lower end of
 200 the concentration range.
 201

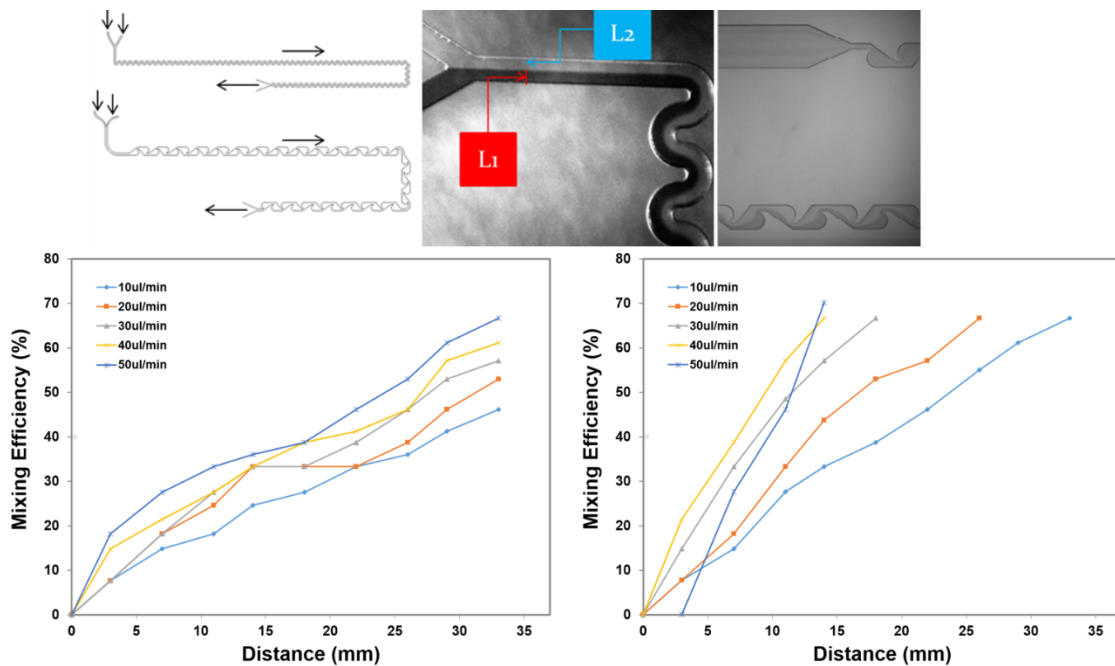
202 B. Optimisation of the Sample Preparation Procedure

203 Sample processing is often the most challenging part of a monitoring solution. For our device, two
 204 critical tasks were considered: the efficacy of the mixing of the reagents with the sample and the
 205 efficiency of the lysis process.

206 Fluid flows are generally laminar in microfluidic devices and mixing occurs primarily by diffusion,
 207 which tends to occur over long distances. Therefore mixing can be enhanced by splitting and
 208 laminating the flow or by introducing recirculating flows, thereby effectively reducing the diffusion
 209 length [25]. Two configurations of mixers were investigated as shown in Figure 5: the serpentine
 210 mixer consisting of 161 meandering turns and the Tesla mixer [26]. The mixing efficiency was
 211 investigated in the serpentine mixer by observing under a microscope the mixing of a dark liquid dye
 212 and a clear liquid as shown in Figure 5B. From this figure, the distances L_1 and L_2 are defined as the
 213 width of each of the two liquids within the channel, when it is possible to discern the boundary from
 214 imaging The mixing efficiency can therefore be calculated using the equation $\eta = (L_1 - L_2) / L_1$ with L_1
 215 and L_2 indicated in Figure 5B. The mixing efficiency was plotted as a function of distance from the
 216 mixer inlet for 5 different flow rates in the 10-50 $\mu\text{L}/\text{min}$ range (Figure 5C and D). As it was not
 217 possible to distinguish the mixed and unmixed zones above 70% only the first part of the mixer
 218 structure was examined (35 mm of length for the serpentine design). The Tesla mixer design
 219 displayed an increased mixing efficiency compared with the serpentine, reaching a 70% mixing
 220 efficiency after just a 15 mm distance from the inlet at high flow rates. An additional advantage is
 221 the lower fluidic resistance in the channel (Figure 5C and D). Note that the mixing efficiency

222 increases for higher flow rates for both mixing designs. The mixing distance required is shorter than
 223 that reported for the seawater ATP analyser, which utilises a serpentine channel length of 133mm
 224 for the mixing of lysis reagent and sample at the end of which the luminescence reagents are added
 225 and then allows a straight channel distance of 350mm until the bioluminescence is measured. The
 226 mixing in a straight channel is ascribed to the asynchronous operation of their peristaltic pumps
 227 causing pulsation [17]. Shorter mixing reduces device footprint.

228



229

230 Figure 5. A) Top left - Design of the two different mixing channel structures (top –serpentine; bottom
 231 – Tesla). B) Top right - Images from the mixing experiments. C) Bottom left - Mixing efficiency for the
 232 serpentine design. D) Bottom right - Mixing efficiency for the Tesla layout.

233

234 C. Device Performance with Varying Types of Water

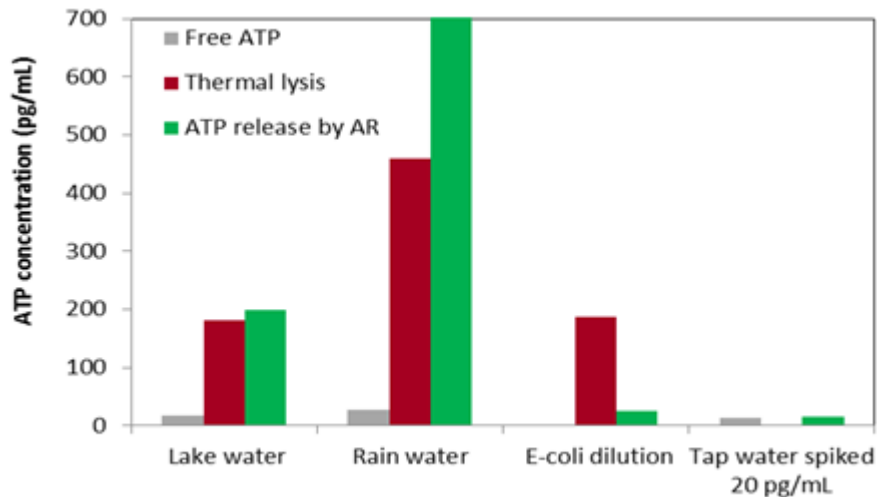
235 Further work was undertaken to quantify the total and free ATP in a variety of water types. The
 236 performance of two different lysis approaches was also carried out with these water types as shown
 237 in Figure 6. The previously generated calibration curve was utilised to convert signal into ATP
 238 concentration, although this does not account for any impact of the water type on ATP
 239 measurement performance. While chemical lysis was shown to provide good output signals, as
 240 shown in Figure 6, problems were observed with channel clogging due to the lysis agent interacting
 241 with the luciferin-luciferase reagents (Figure S3). Fukuba *et al* employed EDTA to avoid issues of
 242 precipitation [17]. As an alternative, thermal lysis was incorporated into the system and trialled.
 243 Preliminary data for a calibration standard of 100 pg/mL suggests that no damage or destruction of

244 the ATP has occurred during the thermal lysis step. Moreover similar RLU as the chemical lysis
245 experiments is demonstrated, with measurements of free (without lysis) and total (with lysis) ATP
246 almost identical (Figure S4). This data also indicates that thermal lysis is successful since the signal
247 for total ATP was higher than the signal for free ATP in the *E. coli* suspension and the tap water,
248 meaning that the thermal lysis extracted ATP from the cells in these samples.

249 Free and total ATP signals were however also similar for the diluted wastewater sample (Figure S4).
250 This result suggests that either thermal lysis did not successfully extract ATP from the cells, or that
251 the extracted ATP was consumed before the analysis, due to either the different water matrix or the
252 different types of microorganisms present in each sample.

253 For surface water, rainwater and tap water total ATP was consistently higher than free ATP as shown
254 in Figure 6, suggesting the thermal lysis efficiency problem was specific to wastewater (Figure S4)
255 and requires further investigation in relation to the components in the wastewater. For surface
256 (lake) water, thermal and chemical lysis were equally effective whereas the tap water sample
257 showed variation between Figure 6 and Figure S4 in terms of the effectiveness of thermal lysis.
258 However, when analysing rainwater samples, chemical lysis outperformed the thermal approach in
259 terms of the level of total ATP measured. The rainwater ATP were high though the sample was
260 stored in a collection tank for 3 weeks before processing, and so this data could indicate possible
261 contamination of the storage tank. An *E. coli* dilution, included as a control, showed the opposite
262 trend whereby thermal lysis gave a much higher detection of total ATP. This data confirms that
263 sample preparation steps are challenging to optimise for waterborne pathogen detection and that
264 universal approaches, for all pathogens and all water types, can be difficult to develop. Other
265 microfluidic approaches to ATP detection have used either chemical or thermal lysis and have not
266 compared the performance. A paper based system for *Salmonella* detection utilised boiling of the
267 sample as the sample processing steps were undertaken external to the device; this system is cheap
268 and disposable but not suitable for online early warning applications [19]. Otherwise, the
269 microfluidics systems reported have utilised chemical lysis. Potentially problems relating to the
270 interaction of the lysis reagents and particle formation were avoided, even in wastewater samples,
271 in iFAST system due to the use of magnetic beads for specific pathogen capture and washing [18].

272



273

274 Figure 6. ATP released from the cells by chemical and thermal lysis methods in different types of
 275 water. Free ATP is the ATP measured without any releasing step.

276

277 IV. Conclusions

278 This article presented the development of a microfluidic system acting as an online early warning
 279 system for measuring microbial contamination in drinking water samples through quantification of
 280 ATP. In terms of detection, system operation with regards to flow rate, temperature and reagent
 281 amount were optimised. Highly linear calibration curves for both total and free ATP were
 282 determined, estimating the limit of detection to be better than 2.5 pg/mL; a result which is
 283 comparable to benchtop studies and one previously reported microfluidic set-up.

284 For the sample preparation part of the platform, mixing design was optimised with a Tesla layout
 285 shown to provide a high mixing efficiency over a short channel length with low fluidic resistance.
 286 Different lysis protocols were trialled and efficiency was shown to depend upon the type of water
 287 sample.

288 Overall the developed prototype system demonstrates highly sensitive rapid detection of bacterial
 289 contamination in drinking water samples. Future work should concentrate on further investigating
 290 the impact of water type on lysis efficiency and consideration of the potential to link with
 291 immunomagnetic separation to provide microorganism specific information as well as online testing
 292 of the system within drinking water networks.

293

294 Supplementary Material

295 See supplementary material for further images of the system (Figure S1), the raw data time course
296 for calibration (Figure S2), the clogging observed with chemical lysis (Figure S3) and the preliminary
297 thermal lysis data (Figure S4).

298

299 Acknowledgements

300 All authors of this article acknowledge the financial support of the European Union through the FP7-
301 Integrated Project entitled “Aquavalens” (grant number 311846, theme KBBE-2012-2.5-01).

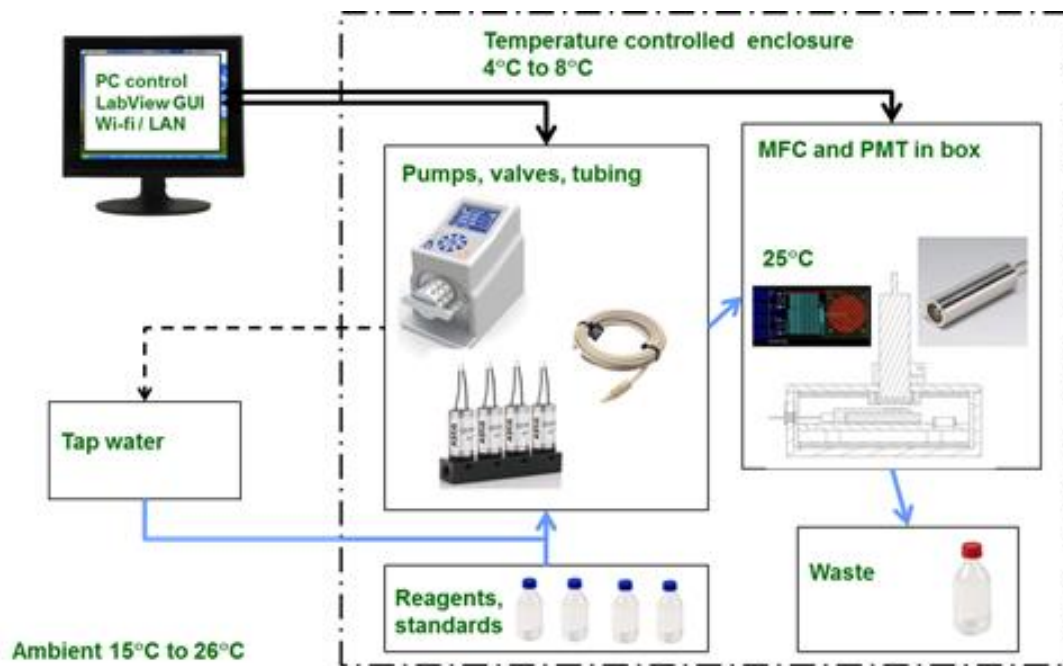
302 References

- 303 1. Storey, M.V., B. van der Gaag, and B.P. Burns, *Advances in on-line drinking water quality*
304 *monitoring and early warning systems*. Water Research, 2011. **45**(2): p. 741-747.
- 305 2. Tryland, I., et al., *On-Line Monitoring of Escherichia coli in Raw Water at Oset Drinking Water*
306 *Treatment Plant, Oslo (Norway)*. International Journal of Environmental Research and Public
307 Health, 2015. **12**(2): p. 1788-1802.
- 308 3. Delahaye, E., et al., *An ATP-based method for monitoring the microbiological drinking water*
309 *quality in a distribution network*. Water Research, 2003. **37**(15): p. 3689-3696.
- 310 4. Bridle, H., B. Miller, and M.P.Y. Desmulliez, *Application of microfluidics in waterborne*
311 *pathogen monitoring: A review*. Water Research, 2014. **55**: p. 256-271.
- 312 5. Banna, M.H., et al., *Online Drinking Water Quality Monitoring: Review on Available and*
313 *Emerging Technologies*. Critical Reviews in Environmental Science and Technology, 2014.
314 **44**(12): p. 1370-1421.
- 315 6. Buyschaert, B., et al., *Online flow cytometric monitoring of microbial water quality in a full-*
316 *scale water treatment plant*. npj Clean Water, 2018. **1**(1): p. 16.
- 317 7. Hojris, B., et al., *A novel, optical, on-line bacteria sensor for monitoring drinking water*
318 *quality*. Scientific Reports, 2016. **6**: p. 23935.
- 319 8. Pinto AJ, et al., *Spatial-temporal survey and occupancy-abundance modeling to predict*
320 *bacterial community dynamics in the drinking water microbiome*. mBio, 2014. **53**(3): p.
321 e01135-14.
- 322 9. Simões, J. and T. Dong, *Continuous and Real-Time Detection of Drinking-Water Pathogens*
323 *with a Low-Cost Fluorescent Optofluidic Sensor*. Sensors (Basel, Switzerland), 2018. **18**(7): p.
324 2210.
- 325 10. Vang, Ó.K., et al., *Evaluation of ATP measurements to detect microbial ingress by wastewater*
326 *and surface water in drinking water*, in *Water Research*. 2014. p. 309-320.
- 327 11. Sherchan, S., et al., *Near Real-Time Detection of E. coli in Reclaimed Water*. Sensors 2018.
328 **18**: p. 2303.
- 329 12. Fukuba, T., et al., *A microfluidic in situ analyzer for ATP quantification in ocean*
330 *environments*. Lab on a Chip, 2011. **11**(20): p. 3508-3515.
- 331 13. <https://www.applitek.com/products/ez-atp>.
- 332 14. Bridle, H., et al., *Detection of Cryptosporidium in miniaturised fluidic devices*. Water
333 Research, 2012. **46**(6): p. 1641-1661.
- 334 15. Liu, B.-F., et al., *Microfluidic Chip toward Cellular ATP and ATP-Conjugated Metabolic*
335 *Analysis with Bioluminescence Detection*. Analytical Chemistry, 2005. **77**(2): p. 573-578.
- 336 16. Lee, S.J., et al. *Microfluidic ATP-Bioluminescence Sensor for Detection of Airborne Microbe*.
337 in *TRANSDUCERS 2007 - 2007 International Solid-State Sensors, Actuators and Microsystems*
338 *Conference*. 2007.

- 339 17. Fukuba, T., et al., *Adenosine Triphosphate Measurement in Deep Sea Using a Microfluidic*
340 *Device*. *Micromachines*, 2018. **9**(8): p. 370.
- 341 18. Ngamsom, B., et al., *A Microfluidic Device for Rapid Screening of E. coli O157:H7 Based on*
342 *IFAST and ATP Bioluminescence Assay for Water Analysis*. *Chemistry – A European Journal*,
343 2017. **23**(52): p. 12754-12757.
- 344 19. Jin, S.-Q., et al., *A cost-effective Z-folding controlled liquid handling microfluidic paper*
345 *analysis device for pathogen detection via ATP quantification*. *Biosensors and Bioelectronics*,
346 2015. **63**: p. 379-383.
- 347 20. Hammes, F., et al., *Measurement and interpretation of microbial adenosine tri-phosphate*
348 *(ATP) in aquatic environments*. *Water Research*, 2010. **44**(13): p. 3915-3923.
- 349 21. Vang, O.K., et al., *Evaluation of ATP measurements to detect microbial ingress by wastewater*
350 *and surface water in drinking water*. *Water Research*, 2014. **64**: p. 309-320.
- 351 22. Vang, O.K., *ATP measurements for monitoring microbial drinking water quality*. 2013, Kgs.
352 Lyngby: Technical University of Denmark.
- 353 23. Guardigli, M., A. Lundin, and A. Roda, *"Classical" Applications of Chemiluminescence and*
354 *Bioluminescence*. *Chemiluminescence and Bioluminescence: Past, Present and Future*, ed. A.
355 Roda. 2011: Royal Soc Chemistry, Thomas Graham House, Science Park, Cambridge Cb4 4wf,
356 Cambs, Uk. 143-190.
- 357 24. Ford, S.R. and F.R. Leach, *Bioluminescence methods and protocols, in Improvements in the*
358 *application of firefly luciferase assays*. 1998, R. A. Larossa, Humana Press Inc.: Totowa, NJ.
- 359 25. Lee, C.-Y., et al., *Microfluidic Mixing: A Review*. *International Journal of Molecular Sciences*,
360 2011. **12**(5): p. 3263-3287.
- 361 26. Hong, C.-C., J.-W. Choi, and C.H. Ahn, *A novel in-plane passive microfluidic mixer with*
362 *modified Tesla structures*. *Lab on a Chip*, 2004. **4**(2): p. 109-113.

363

364



366

367

368

369

370

371

372

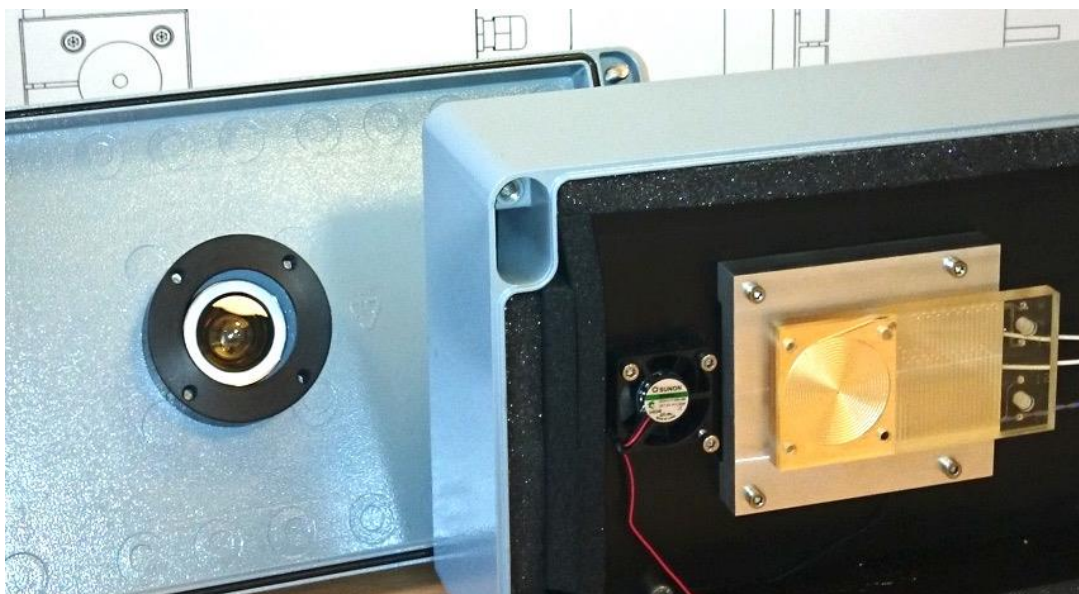
373

374

375

376

377



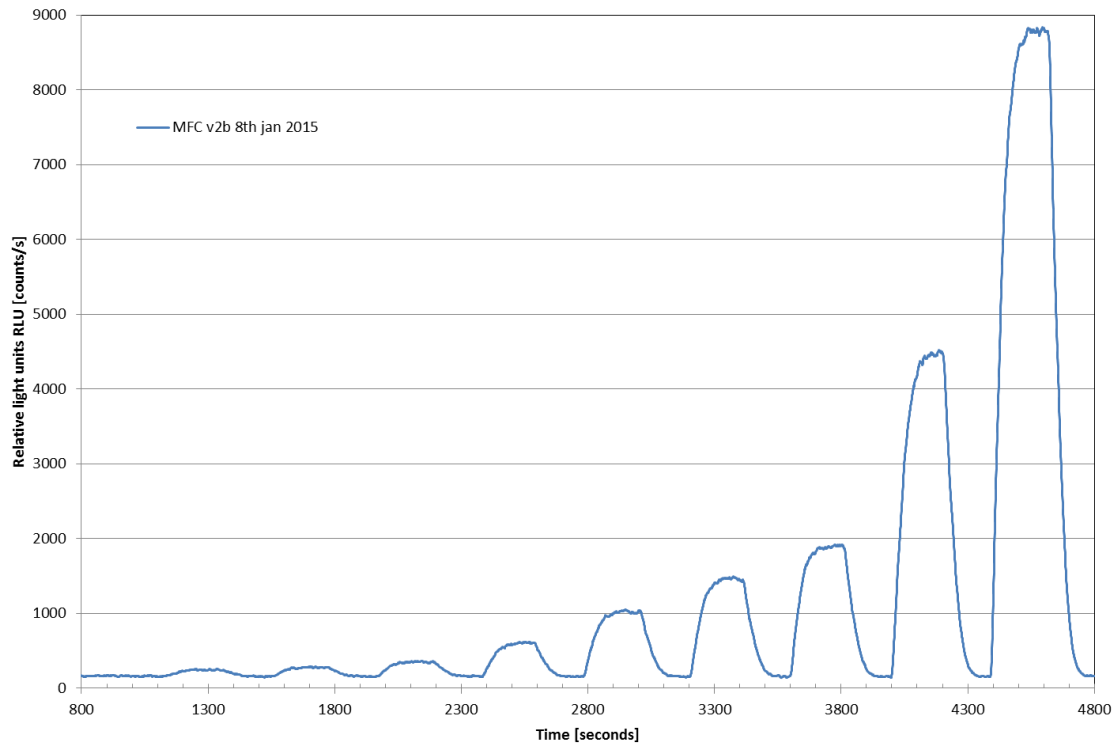
378 Figure S1

379 Upper image: A functional schematic of the concept of the ATP platform. A local computer controls
 380 the instrumentation needed to configure and perform the online ATP measurements. The
 381 instrumentation consists of programmable pumps, controllable valves and a PMT detector assembly
 382 that includes the microfluidic based assay. A dedicated graphical user interface (GUI), based on
 383 LabView®, allows access to work with the system. Data transfer requires connectivity to the internet
 384 using either a WiFi- or LAN connection. Fluidic connections for liquids are shown using blue arrows.
 385 The temperature controlled enclosure ensures the stability of reagents regardless of local conditions
 386 and seasonal variations in ambient temperatures. The measurements are performed on the

387 microfluidic cartridge using a highly sensitive photomultiplier tube both mounted in a box in order to
388 exclude external light.

389 Lower image: The head of the PMT is fixed in the lid on the left side of the picture. The MFC is placed
390 on the temperature controlled aluminium plate in the right side of the picture. The fan visible next
391 to the aluminium plate is used to recirculate the air to maintain a constant temperature throughout
392 the interior of box. Notice the black foam insulation at the rim of the box providing thermal
393 insulation.

394



395

396 Figure S2

397 Raw data obtained with ATP-spiked samples using the following concentrations measured in pg/mL
398 (left to right) 2.5, 5, 10, 25, 50, 75, 100, 250, 500.

399

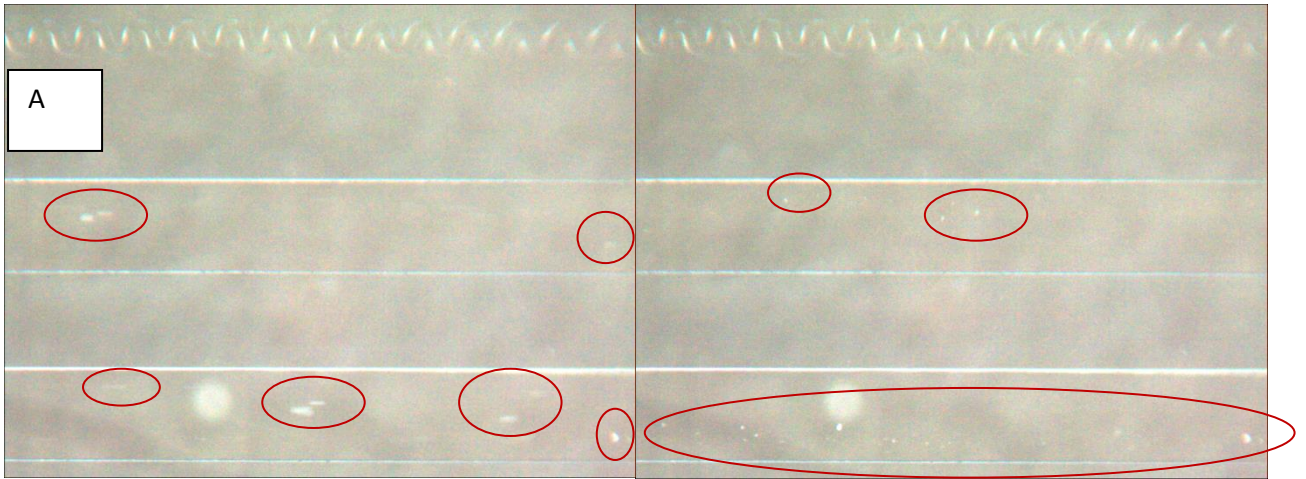
400

401

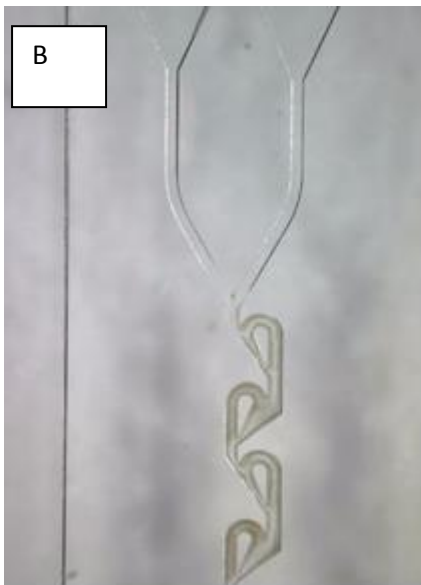
402

403

404



405



406

407

408

409

410

411

412

413 Figure S3

414 A: Formation of particles in the microfluidic when ATP free water, lysis reagent and LL are supplied in
415 the three inlet channels. Left panel shows that particles are moving when the flow is on and right
416 panel shows that these particles deposit in the channels when the flow is turned off. The red circles
417 highlight the areas where particles are observed.

418 B: The left photo shows two clear liquids merging with particulate matter developing downstream in
419 the Tesla mixer structure. On the right picture solid matter can be seen to deposit in the slower

420 flowing regions of the mixer. In the spiral readout region larger agglomerates of the solid matter has
421 formed while flowing downstream.

422 C: Formation of particles when mixing ATP free water, lysis reagent and LL in a cuvette results in a
423 turbid liquid (left picture). Picture is taken immediately after mixing the reagents. Mixing of LL with
424 the ATP free water in a cuvette does not generate particles, but the mixture remains clear (right
425 picture).

426

427

428

429

430

431

432

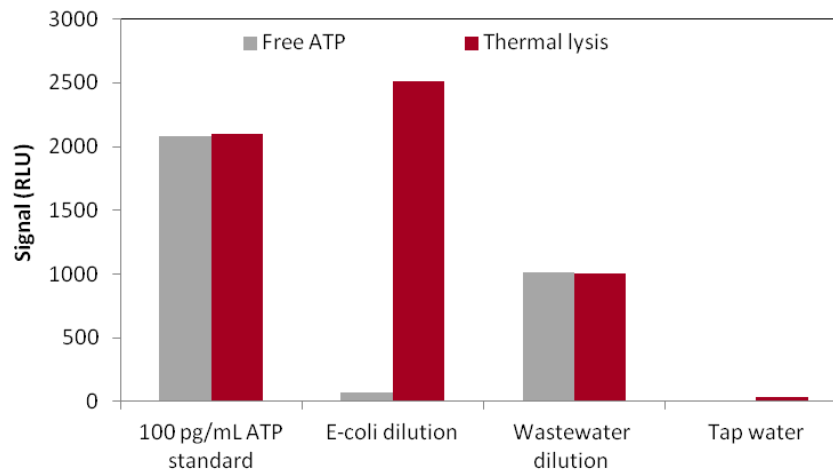
433

434

435

436

437



438 Figure S4. Preliminary investigations of the performance of thermal lysis. The wastewater was
439 sourced at DTU and diluted 100 times before use in the device.